land

MDPI

Article

First Evidence of Roman Gold Mining Obtained by Luminescence Dating of Sediments in Les Guilleteres D'All (Cerdanya, Girona, Eastern Pyrenees)

Jorge Sanjurjo-Sánchez [1,*], Jordi Morera Camprubí [2] and Oriol Olesti Vila [2]

[1] University Institute of Geology, University of A Coruña, 15008 A Coruña, Spain
[2] Universitat Autónoma de Barcelona, Bellaterra, 08193 Barcelona, Spain; jordi.morera@uab.cat (J.M.C.); oriol.olesti@uab.cat (O.O.V.)
* Correspondence: jorge.sanjurjo.sanchez@udc.es; Tel.: +34-881012695

Abstract

In recent years, evidence of gold mining during the Roman period has been found by archaeologists in the Cerdanya region (Girona, Catalonia). In this region, Les Guilleteres d'All has been described as a mining complex because of the erosive features observed in the landscape; surveys have identified hydraulic mining opencast structures named chantier-cirques and chantier-ravins. The latter are smaller, but both require a water reservoir, specifically a water retention facility, to supply water flow. One of these buried water reservoirs has been excavated, revealing an enlarged area with a dam constructed from stone blocks. Two pottery sherds were found within the sediment layers deposited on the bottom of the reservoir—one dated to the 1st–2nd c. AD and the other to the Bronze Age—indicating that the reservoir was filled during historical times and the nearby presence of settlements from these periods. Optically Stimulated Luminescence (OSL) dating was performed on two waterlain sediment layers deposited at the bottom deposited at the reservoir. The obtained ages, dating to 2nd–4th c. AD, correspond to the final phase or abandonment of mining activities. Hence, these ages provide the first evidence of mining activities in Les Guilleteres during Roman times.

Keywords: OSL dating; luminescence dating; gold mining; eastern Pyrenees; Roman mining; Cerdanya

Academic Editor: Francesca Cigna

Received: 2 May 2025
Revised: 9 September 2025
Accepted: 10 September 2025
Published: 19 September 2025

Citation: Sanjurjo-Sánchez, J.; Morera Camprubí, J.; Vila, O.O. First Evidence of Roman Gold Mining Obtained by Luminescence Dating of Sediments in Les Guilleteres D'All (Cerdanya, Girona, Eastern Pyrenees). *Land* **2025**, *14*, 1912. https://doi.org/10.3390/land14091912

1. Introduction

Roman mining landscapes have been studied intensively in several regions of Europe and northern Africa: northwestern and southern Spain, Dacia-Rumania, central Gaul, Britain, Egypt, etc. [1]. In particular, gold exploitation in northwestern Spain has generated a significant amount of research studying the numerous mines in this region, as it is considered one of the most important areas of gold extraction within the Roman Empire; the most notable example is Las Médulas, where the hydraulic technique, described by Pliny as ruina montium, was employed [2]. In other regions, there are also examples of smaller Roman mining landscapes where water power was used. One instance is the Oriental Pyrenees area, specifically the Cerdanya region (Girona, Catalonia), where we have conducted extensive archaeological research over the last 15 years, identifying the remains of an alluvial gold mine opencast in the "Les Guilleteres d'All" area [3].

1.1. Historical Background

The Cerdanya is a Pyrenean territory formed by a large plain, located 1200 m. above sea level, and the surrounding mountains are up to 2900 m. high (Figure 1). In antiquity, it was occupied by a local Iberian tribe, called Cerretani in ancient literary sources (Strabo 3.4.11, Pliny, NH 3.4.5). They were an Iron Age community living in small-scale hillforts (oppida), exploiting the agriculture and livestock resources of this mountain area. They knew of the existence of alluvial gold in the region, and during the 3rd–2nd c. BC crafted naviform gold earrings, as evidenced by discoveries at the currently excavated oppida of Castellot and Tossal de Baltarga [4]. The Romans occupied the Oriental Pyrenees around the mid-2nd c. BC, establishing garrisons (praesidia), controlling the former indigenous oppida and exploiting several local resources such as livestock, pastures and metals. The exploitation of Pyrenean gold, along with other metals such as silver or lead, is mentioned by Pliny the Elder (Pliny NH 4, 112, 7–8 [5]). Our excavations at the site of El Castellot (Bolvir), the main oppidum of the region, identified a complex poly-metallurgical workshop, with evidence of artificial gold, silver, lead and cinnabar production [5]. This workshop must be connected to the presence of a military Roman garrison at the site, as the Romans were the only ones who could manage the use of alloys like brass or cinnabar, indicated by the scarce presence of these alloys in the 2nd. c. BC Hispania.

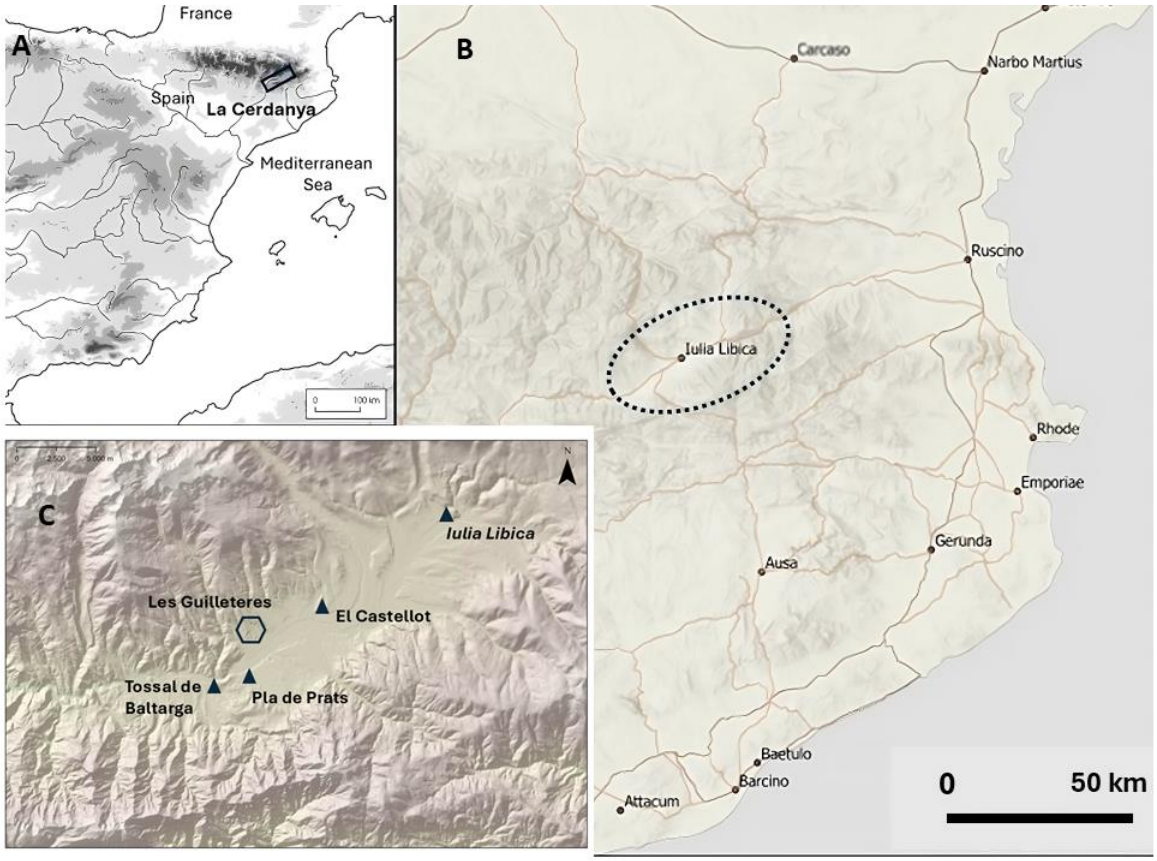

Figure 1. Location of Les Guilleteres (hexagon) in Cerdanya, Girona, Catalonia (Spain). (**A**) General map, (**B**) regional map and (**C**) location of Les Guilleteres. Triangles correspond to archaeological locations.

These data are reinforced by two other ancient literary sources. The first is the rich booty taken by Cn. Domitius Calvinus from the Cerretani in 39 BC, following his suppression of an uprising. Dio Cassius explicitly mentions that the gold came from the local population (DC 48.42). The second reference comes from Martial (Ep. 6.86), which contains

a subtle mention of the gold produced in this region (*Libicas messis*) in connection with Iulia Libica, the Roman municipium founded in Cerdanya [5,6].

1.2. Geographical and Geological Context

Les Guilleteres d'All is a mining complex located on the northeastern flank of the Cerdanya Valley, lying in the piedmont of the Catalan Axial Pyrenees. The Segre River flows 1.5 km south of the southernmost mine. The elevation within the studied area ranges from 1084 m to 1455 m above sea level (see Figure 2). The mining landscape is roughly 11.5 km^2, encompassing the municipalities of Ger, Olopte and All [3], and spans five different mining zones [7] (see Figure 3). These mining zones can be initially discerned via aerial imagery, as ravines expose, without arboreal vegetation, the eroded geological layers of clay and marl. Various excavated trenches in these structures converge into a main trench, forming a distinctive pattern. These are geological formations associated with Roman hydraulic opencast mining, only known from Roman period operations, as highlighted in the works of Claude Domergue [2]. Furthermore, the erosion patterns observed in these gulches do not follow the natural slope orientation of the terrain but an oblique one, indicating an anthropic origin. Gold is found in secondary alluvial deposits at Les Guilleteres [4]. Eroding streams descending from the Pyrenees transported auriferous particles, which accumulated in alluvial terraces during the Miocene. These alluvial terraces at Les Guilleteres consist of sedimentary brown clay and reddish-yellow marls. Beneath this sedimentary auriferous layer lies bedrock composed of slate and schist, which constitutes the principal geological formation of the entire Pyrenean region [8].

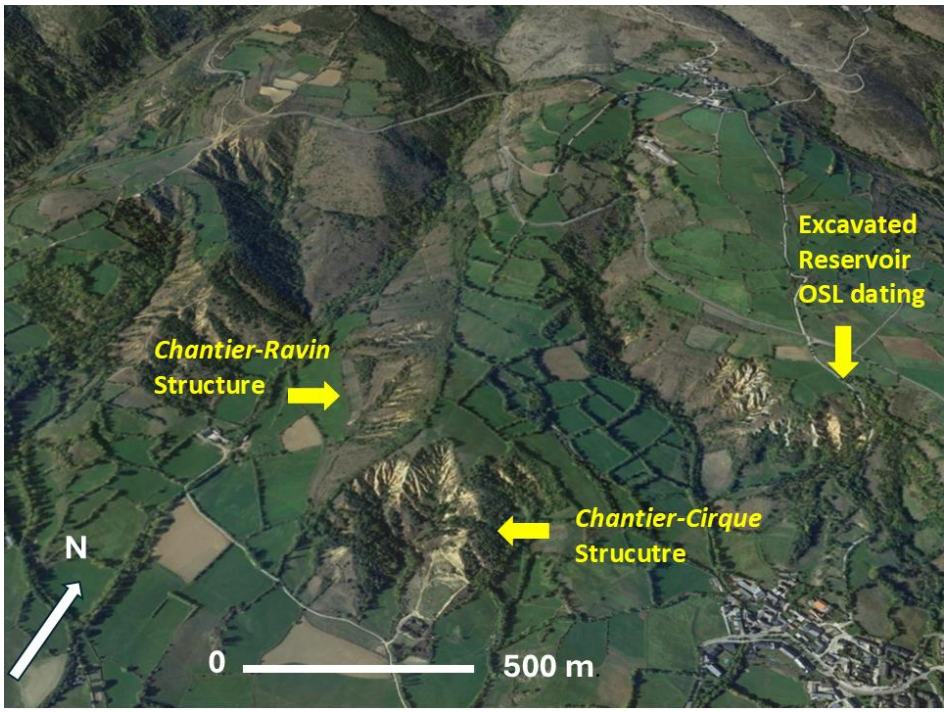

Figure 2. Opencasts ("chantiers") identified and location of the excavated reservoir in Les Guilleteres. Coordinates of the OSL sampling: 2°24′10″ N 1°50′06″ E.

1.3. Previous Research: Geomorphology and Settlement Patterns

Previous surveys at the Les Guilleteres site identified hydraulic mining opencast structures, with some of them named chantier-cirques following Cl. Domergue's terminology and others named chantier-ravins [3]. A chantier-ravin consists of an excavated trench specifically adapted to the slope of the extraction front, taking advantage of the natural slope, which is eroded by a constant or regulated water flow. Additionally, smaller trenches

are excavated and subsequently eroded by water converging into the main channel. This mining structure eroded and washed down the Miocene alluvial terraces, releasing gold-rich grains that were later recovered at the end of the main channel of the chantier-ravin, which is now lost. With the notable exception of two cases, all Roman mining landscapes at Les Guilleteres d'All appear to show this shape of opencast chantier-ravins, as documented by A. Soto [7].

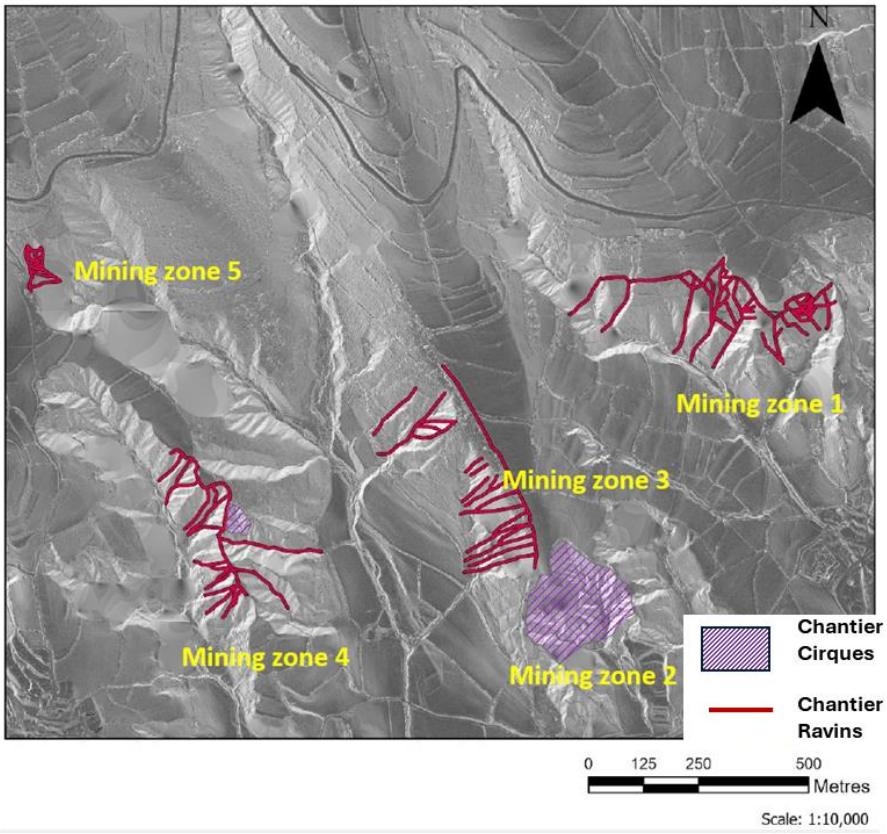

Figure 3. Details of the Roman hydraulic network and opencasts at Les Guilleteres [7]. Metadata: reclassified hillshade and slope imagery derived from LIDAR data. ETRS89 31N.

The other typology of deep opencasts or chantiers detected in Les Guilleteres is the chantier-cirque. The largest example of a chantier-cirque is in mining zone 2 (Figure 3). The chantier-cirque is a mining extraction front that is considerably larger than the chantier-ravin. It has an almost circular shape (about 300 m in diameter) and is exploited from the bottom upward, developing quasi-vertical sides approximately 20–30 m high. Trenches eroded by water are excavated in all directions, converging at the centre of this semicircle. It requires at least one water reservoir, normally situated at the top, to supply the flow, along with distribution channels around its perimeter. The volume of earth extracted in Les Guilleteres has been estimated at 2 million m^3, which, while impressive, is lower than other mines, where the volume extracted can reach up to 20 million m^3 (Figure 3).

From a geomorphological point of view, these structures can be clearly interpreted as gold mines, as they present hydraulic patterns similar to other well-known gold mines; however, definitive dating is missing. Only the archaeological excavation of a hydraulic structure and dating can confirm the function and chronology.

Nevertheless, there are archaeological indicators that provide an indirect chronology. One of them is the existence of the Roman city of Iulia Libica, located about 12 km east of "Les Guilleteres". The monumental forum of the city is a good indicator of the wealth of the local elites during the 1st c. AD [9].

The second indicator is the identification of a rich Roman necropolis (Pla de Prats) located 3 km southwest of the mines [10]. It was located close to the mouth of the natural water drainage coming from the Guilleteres. In the necropolis, two main tombstones were excavated, revealing a monumental mausoleum with an epigraphical display that contained two incinerations. In one tomb, the remains of a Roman horseman, likely a military veteran, were found. In the second one, a magnificent gold bracelet decorated with animal motifs was found, weighing 23 gr. of gold, which is an unusual amount of metal, especially in a mountain area. The existence of the mausoleum points to a large settlement, perhaps a vicus connected to the mines, instead of a private villa or a rural residence. The location close to the mines and the presence of a gold bracelet could reinforce the Roman chronology of gold exploitation.

2. Previous Excavation of the Water Reservoir

In order to obtain chronological data for the eroded structures of "Les Guilleteres", we conducted several geophysical and archaeological surveys in mining sector 1. We identified an old channel coming down the slope, ending in an enlargement, which we interpreted as a possible reservoir. Two trenches were opened in the suggested reservoir. One trench was opened during excavations between 2010 and 2012, and a second trench during a 2019 campaign. During the first campaign, our team excavated the southern part of this water reservoir (T1). The excavation successfully identified a section of the reservoir and the mentioned incoming channel (Figure 4).

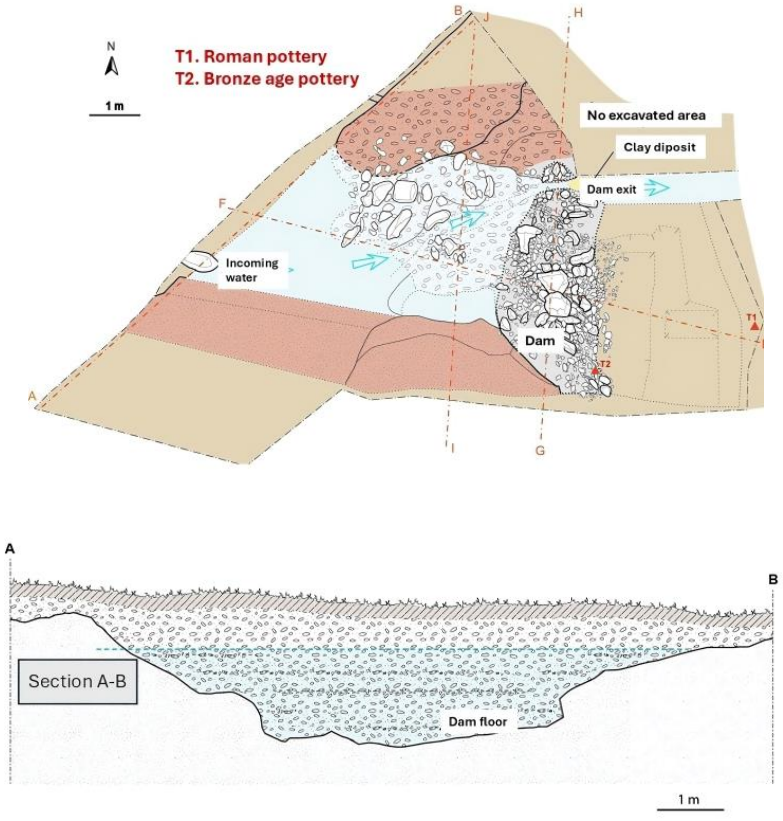

Figure 4. Plan of the water reservoir excavated in 2010–2012 [3], including one of the stratigraphic section drawing (A-B).

The excavated ditch measured 4.5 m in width with a maximum depth of 1.5 m. The preserved ditch was 0.6 m high from the bottom of the reservoir, and a dam was constructed

with stone blocks measuring, on average, 50–60 cm on one side, while the ditch's edges were made of smaller stone blocks measuring, on average, 15–30 cm on one side (Figure 5).

Figure 5. Image of the excavated dam in 2010–2012 with some of the large stone blocks [3].

The reservoir ground followed the natural slope of 15% in a north–south direction. It is important to note that this represents only a section of a largely unknown reservoir stretching to the north, and it was probably not the only one, as further west, more opencasts would have required additional water tanks. During the 2019 campaign, we opened a new sector of the water reservoir, 6 metres upslope, identifying again the remains of the same reservoir [3]. During the 2012 excavation, we found two pottery sherds within the sediment layers deposited on the bottom of the reservoir. One sherd was dated to the Early Roman Empire period (1st–2nd c. AD) based on the typology of the vase and macroscopic fabric analysis. The second one belonged to the Bronze Age, indicating the filling of the water reservoir during historical times and the nearby presence of settlements from this period. Due to the scarcity of pottery sherds, we decided to determine the absolute ages using Optically Stimulated Luminescence (OSL) dating of the sediment layers.

3. Study Aim

In order to accurately determine the age of the sediment infill in the excavated basin at Les Guilleteres and verify if the water reservoir was associated with Roman gold mining, two sediment samples were dated using OSL. In September 2022, we opened a new trench in the reservoir (Figures 6 and 7), three metres from the old section opened in 2012 (so called trench 5), upslope, with the help of a mechanical digger, obtaining a new and untouched section of the sediments filling the reservoir. The trench was 2 m wide to allow for the study of this section. The stratigraphy of this section allowed for the identification of the water reservoir boundary, corresponding to the contact between the sediment infill and the Miocene bedrock. The base of the reservoir was located at a depth of 2 m. This was the place where the two sediment samples were obtained for OSL dating (Figure 8). Two fine-grained sediment samples were taken from the walls of the ditch that corresponds to the sedimentary sequence. The dating of these two samples could constitute the first direct evidence of extractive activity in the area, which, along with the rest of the evidence, could confirm that mining activity occurred during the high Roman imperial period.

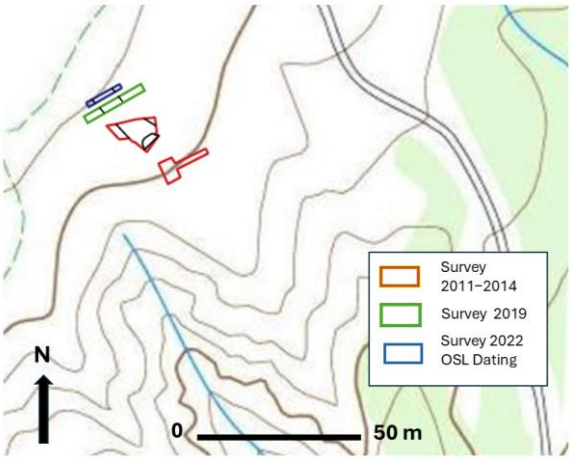

Figure 6. Location of the different surveys and archaeological works developed in "Les Guilleteres". In blue, the survey of 2022 (trench 5). Coordinates of the surveys and OSL sampling: 2°24′10″ N 1°50′06″ E.

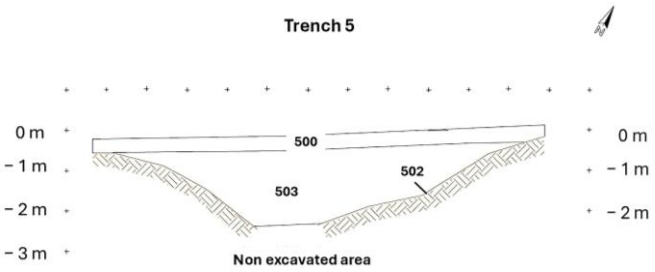

Figure 7. Section drawing of the 2022 survey.

Figure 8. Trench opened for OSL sampling with location of the sampled layers (**A**) and hole of the tube of sample Cerdanya-1 (**B**). The arrows indicate the sampling points for OSL dating.

Luminescence Dating

Luminescence dating, a technique used to date sediments, has become increasingly utilised over the past 25 years. Its use for dating has expanded to almost all types of natural and anthropogenic sediments, making it widely applied in archaeology [11–13]. Specifically, Optically Stimulated Luminescence (OSL) is used, which allows for determining

the age of sediment burial. This is achieved by measuring the accumulated charge in the quartz of the sediment due to its exposure to natural ionising radiation. This is estimated as the equivalent dose (D_e). The ionising radiation comes from the emission of alpha and beta particles and gamma radiation produced by the presence of primordial radioisotopes (from the decay chains of ^{238}U and ^{232}Th and mainly ^{40}K) present in the sediment minerals. Cosmic radiation reaching the Earth's surface also causes, to a small extent, this accumulation of trapped charge. When the quartz grains in the sediment are exposed to daylight during transport, their charge is released, resetting the luminescence clock to zero; when the grains are buried, charge begins to accumulate again. This allows for determining the age of sediment deposition. Various studies have successfully applied this technique to anthropogenic sediments, such as fills in pits, channels, abandoned structures and stagnant bodies of water [14,15]. However, to the authors' knowledge, there is no reference to OSL dating of mining activities.

4. Materials and Methods

For OSL dating, two 30 cm long and 5 cm wide steel cylinders were hammered into the sediment profiles of the trench dug in the deposit. Samples were taken on the lower fine-grained layers of the deposit originating from the water body, ensuring that they corresponded to the early stages of the dam's use. A sediment sample was also collected from the holes left by the cylinders and placed in plastic bags for radioisotope analyses. The sample Cerdanya-1 was taken on one side (north) of the profile at 1.6 m depth. The sample Cerdanya-2 was taken on the other profile of the trench (south) at 1.8 m depth. The tubes filled with sediment were sealed, and the gamma radiation rate of the sediment was assessed in situ with a gamma-ray spectrometer.

The tubes were opened under subdued red light in the luminescence lab of the University of A Coruña. The outer parts of the sediment cores were removed, and the central part was dried and sieved for quartz purification. After sieving, the medium-sized grains, 180–250 μm, were treated with hydrochloric acid and hydrogen peroxide to remove carbonates and organic matter, respectively. The dried feldspars and heavy minerals were removed via density separation using sodium polytungstate solutions with densities of 2.62 g cm^{-3} and 2.70 g cm^{-3}. The remaining quartz fraction was etched in concentrated hydrofluoric acid (40%) for 1 h to remove any remaining feldspars and the outer layer of quartz grains that corresponds to approximately 10 μm of the quartz surfaces that received an additional alpha dose during burial [16]. Hydrochloric acid was applied again to remove any remaining soluble fluorides, and the grains were then dried. The quartz grains were checked with infrared (IR) stimulation to ensure the absence of minerals other than quartz.

For luminescence measurements, an automated Risø DA-15 TL/OSL reader system was used, equipped with blue light-emitting diodes (LEDs). Blue OSL signals were recorded with a coupled 9235QA photomultiplier tube (PMT). Laboratory doses were given using a ^{90}Sr/^{90}Y beta source emitting a 0.100 ± 0.003 Gy s^{-1} dose to samples of the measured geometry. To estimate the equivalent dose (D_e), the single-aliquot regenerative dose (SAR) protocol was used on small multigrain aliquots (~100 grains) after performing preheat tests, and recovery tests were conducted [17]. The last 4 s of the decay curve were subtracted from the fast component (first 0.4 s) to determine the OSL signal. Aliquots that provided recycling rations below or above 0.9 and 1.1, respectively, were rejected. Preheat tests were performed before SAR measurements, and dose recovery tests were performed later on similar aliquots for 20 discs per sample. Single-grain measurements were also carried out using a Risø DA-22 TL/OSL reader system, equipped with a Hamatsu PMT and a coupled ^{90}Sr/^{90}Y beta source emitting a 0.12 ± 0.003 Gy s^{-1} dose to the grains.

The dose rate (Dr) was estimated using low-background gamma spectrometry on bulk samples. Bulk samples were dried, milled and calcined to 500 °C. before measurements. Marinelli beakers were used, and measurements were taken after radon equilibration in a coaxial Camberra-XTRA gamma detector (Ge-Intrinsic) model GR6022 within a 10 cm thick lead shield. Conversion factors presented by Guerin et al. [18] were used. The alpha contribution was neglected for quartz dose rates, with the beta dose rate being corrected due to the HF etching step. Water content and water saturation values were assessed in the laboratory for all samples to estimate average water content (20 ± 4% for both samples), and the cosmic dose rates were calculated in accordance with Prescott and Hutton [19]. The external dose rates (gamma and cosmic doses) were also measured with a gamma-ray spectrometer (GF Instruments Gamma Surveyor Vario), equipped with a BGO probe ($Bi_4Ge_3O_{12}$) featuring 2018 channels, a 51 mm × 51 mm detector (103 cm^3), probe dimensions of 70 mm in width and 290 mm in length (VB6), and a shielded photomultiplier.

5. Results

The radioisotope activity concentration in the sediments was high for ^{238}U and ^{232}Th decay chains and ^{40}K. This is probably due to the high clay content, as clays are usually rich in such radioisotopes [20]. The obtained values for ^{238}U are around 37 Bq kg^{-1}, while for ^{232}Th, they are around 58 Bq kg^{-1}. ^{40}K concentrations are between 723 ± 30 and 766 ± 30 Bq kg^{-1}. No disequilibrium is observed for ^{238}U and ^{232}Th decay chains. The resulting D_rs are 3.32 ± 0.25 mGy a^{-1} and 3.56 ± 0.18 mGy a^{-1} for samples Cerdanya-1 and Cerdanya-2, respectively (Table 1).

Table 1. Activity concentration of radioisotopes in the studied samples and resulting dose rate (D_r).

Sample	^{238}U (Bq kg^{-1})	^{214}Bi (Bq kg^{-1})	^{232}Th (Bq/kg)	^{40}K (Bq kg^{-1})	D_r (mGy a^{-1})
Cerdanya-1	41 ± 8.5	37.9 ± 1.6	58.8 ± 2.4	723 ± 30	3.32 ± 0.25
Cerdanya-2	39 ± 8.0	37.0 ± 1.5	58.5 ± 2.4	766 ± 30	3.56 ± 0.18

OSL signals were dim and low, but they exhibited a quick decay with a dominant fast signal. About 30% of the OSL signal remains after 1 s of exposure to blue LEDs. The remaining signal is about 17% after 2 s and 8% after 5 s, with the bleaching rate being very similar for both samples (Figure 9). Preheat tests showed a wide plateau for the Des when preheat temperatures between 180 and 240 °C were applied for 10 s before measuring OSL signals (Figure 10). Thus, a 220 °C preheat was performed for 10 s during the SAR measurements, with a cut heat of 200 °C.

The dispersion of the individual aliquots of both samples is different despite the similarity of the grain sizes of both samples. For Cerdanya-1, the aliquots show a low dispersion and skewness (skewness coefficient 0.90), and the abanico plot shows most aliquots around a central value (Figure 11). The high overdispersion value of the central age [21] observed is probably due to the poor signal (74 ± 10%). For Cerdanya-2, a higher dispersion of aliquots is observed (Figure 11), with a skewness coefficient (1.37) significantly lower. Thus, the Central Age Model (CAM) of Galbraith et al. [21] was used to assess the De and age for Cerdanya-1, and the Minimum Age Model (sigma b 0.3) was used to assess both values for Cerdanya-2. The resulting ages are very similar, with the age ranges in agreement (Table 2). The dose recovery test provided recovery rates of 0.97 ± 0.01 and 0.92 ± 0.02, with overdispersions below 5% and around 7 ± 2% for Cerdanya-1 and Cerdanya-2, respectively.

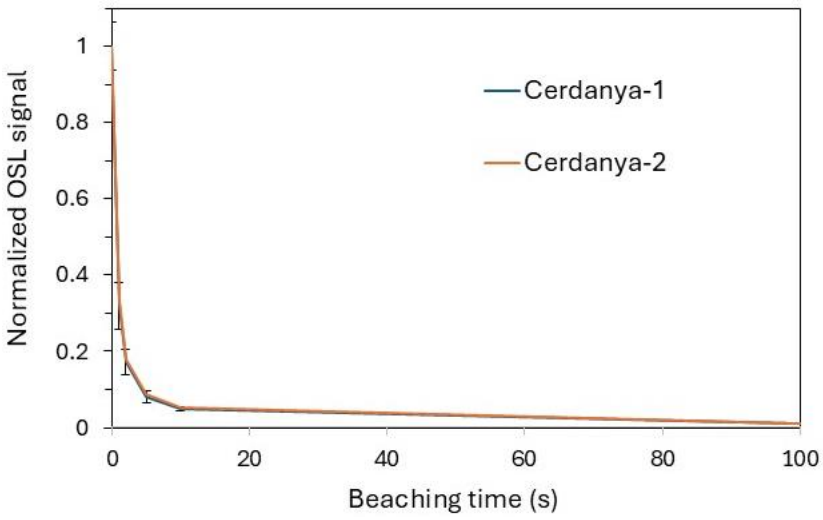

Figure 9. Bleaching test of two samples obtained from average of 5 aliquots per sample.

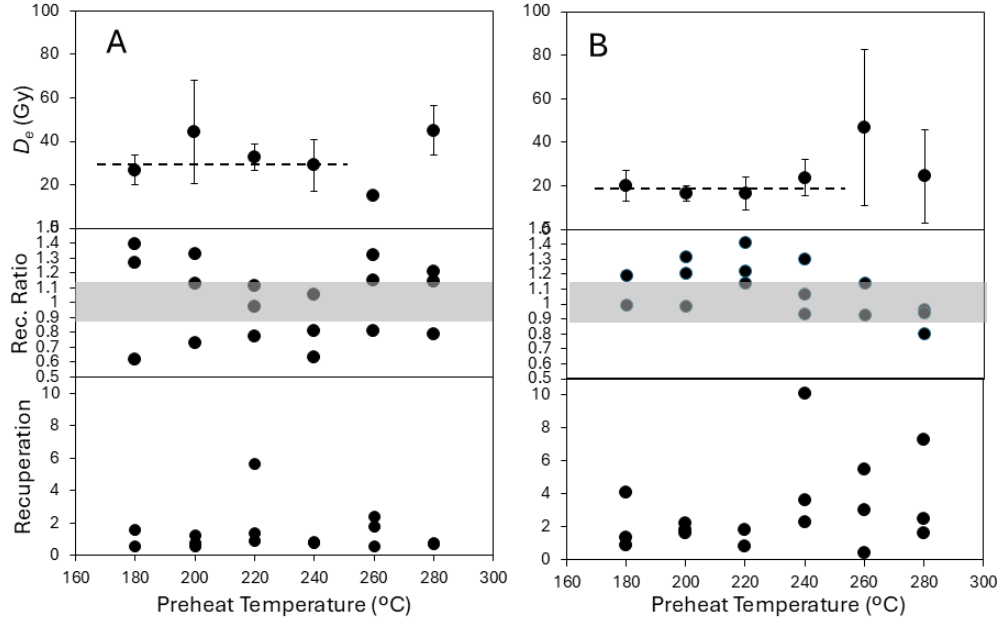

Figure 10. Results of the preheat tests performed for (**A**) Cerdanya-1 and (**B**) Cerdanya-2. The upper plots show the obtained Des at different preheat temperatures. The middle plots show the recycling ratios (shadowed area correspond to acceptable ratios), and the lower plots show the recuperation ratios (in %).

Table 2. Sample depth, number of accepted aliquots (N), method (multigrain aliquots, MG; single-grain, SG), equivalent dose obtained (De). The MAM was used for both Cerdanya-1 MG and SG, and Cerdanya-2 SG, while the CAM was used for Cerdanya-2 MG.

Sample	Depth (m)	Met.	N	D_e (Gy)	Age (y)	Year	Year (as Range)
Cerdanya-1	1.6	MG	37	5.87 ± 0.30	1768 ± 160	255 ± 160 AD	95–415 AD
		SG	97	5.65 ± 0.83	1702 ± 280	321 ± 280	41–610 AD
Cerdanya-2	1.8	MG	35	7.04 ± 0.91	1978 ± 275	45 ± 275 AD	231 BC–320 AD
		SG	33	5.46 ± 0.81	1535 ± 240	488 ± 240	248–728 AD

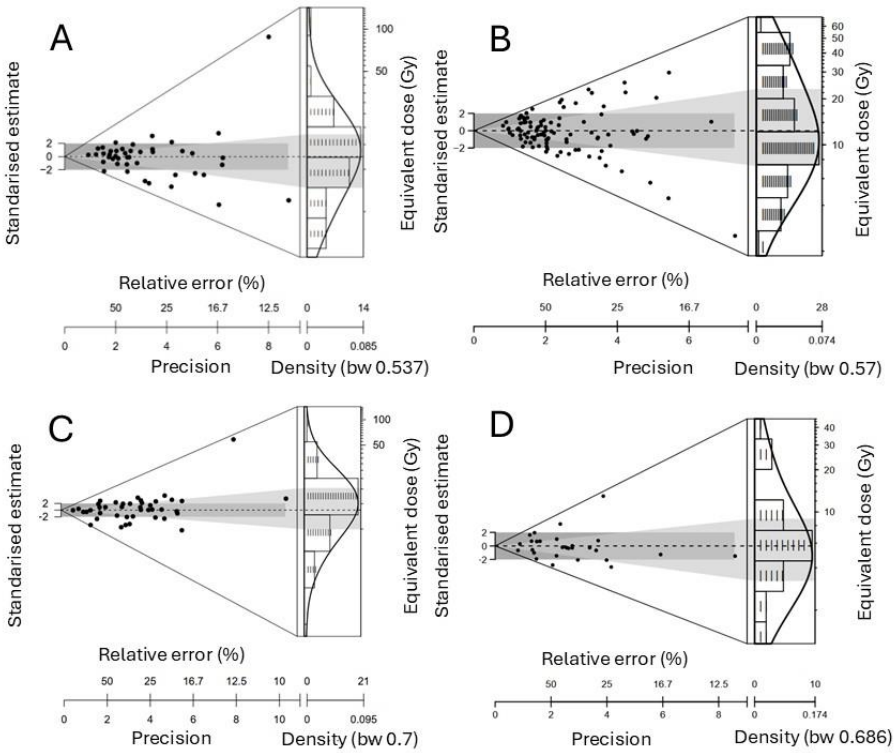

Figure 11. Abanico plots that show the De distributions of multigrain aliquots for Cerdanya-1 MG (**A**) and SG (**B**), and Cerdanya-2 MG (**C**) and SG (**D**).

Given the differences observed using multigrain aliquots in both samples, despite the grains being theoretically transported and deposited under similar conditions, a second set of measurements was carried out on single grains for both samples. A set of 1200 grains was measured for both samples, but the results provided a much higher number of accepted aliquots for Cerdanya-1 (98) than for Cerdanya-2 (33). The resulting De distributions can be observed in Figure 11B,D for Cerdanya-1 and Cerdanya-2, respectively. Both distributions are similar to those obtained for multigrain aliquots, as the Des obtained using the MAM were similar. For Cerdanya-1, both results fit very well, while for Cerdanya-2, the obtained age is slightly lower but not significantly different (1 σ). Thus, both single-grain ages are in agreement (Table 2).

As shown in Table 2, SG measurements provided new Des that were compared to the MG Des and resulting ages. The De distributions (Figure 11) observed for both samples are different. However, the samples were taken from the same sediment layer and the expected ages should be the same. For sample Cerdanya-1 the MAM provides the same result for both MG and SG. However, for sample Cerdanya-2, the resulting age is consistent for SG with the MAM, but not for the CAM with the MG. This difference can be due to grain mixing or an influx or older aged grains. The distribution of aliquots that shows a well-bleached, unmixed sample, and the CAM age obtained with MG for sample Cerdanya-2, provides the only strong evidence of Roman period mining, which is consistent with the MAM age obtained for sample Cerdanya-1

6. Discussion

First, the sediment ages obtained by OSL match the expectations based on literary sources and archaeological evidence: the Roman pottery found previously in the reservoir, the characteristic morphology of Roman gold exploitations, and the contemporary existence of a Roman city and several Roman sites close by. The sedimentation did not necessarily start once the mining activity ceased, and probably increased due to the lack of use of the

water reservoir, which was probably permanently filled. The fine grains of the sediment layers show that they were deposited in stagnant water conditions. However, when the mine was active, the hydraulic system prevented the permanent stagnation of the sediments. Immediately after the abandonment of the exploitation, the hillslope runoff transported the grains, likely being buried after the abandonment, rather than the beginning, of this activity.

The two OSL ages provide a very broad abandonment period, mostly because of the low signal-to-noise ratio. However, the first MG age (Cerdanya-1) dates back to the late 1st c. AD and the early 5th c. AD, while the second one (Cerdanya-2) ranges from the late 3rd c. BC to 4th c. AD. For SG ages, the Cerdanya-1 dates back to the mid-1st c. AD and the early 7th c., and Cerdanya-2 dates back to the mid-3rd c. and the beginning of the 8th c. It was expected that the age of the decommissioning of the channel and the studied deposit must fall within these two ranges, between the late 3rd c. AD and the early 4th c. AD. If we consider the MG age range for Cerdanya-2, spanning from the late 3rd c. BC to the first half of the 2nd c. BC, then these periods can be ruled out for historical reasons; there is no historical or archaeological evidence of the presence of Romans in the studied region, and the local population lacked the means to carry out resource exploitation of this magnitude. However, the SG age fits well with the expected age.

Knowledge of the regional archaeological context can help improve the precision of the chronology for these structures within the age ranges obtained via OSL. As mentioned, gold and silver working in the region has been documented as early as the second half of the 2nd c. BC (Castellot de Bolvir Metallurgical Workshop) [5], although this does not necessarily imply local gold exploitation. It is possible that gold mining already started in this time period, although this would be an early historical application of the hydraulic technique documented in Les Guilleteres.

Despite the lack of a precise date for the onset of the mines, it seems more probable to link the beginning of gold mining in the region to the major transformation of this territory following the foundation of the Roman municipality of Iulia Libica, which is well documented both archaeologically and epigraphically [9,22]. The significant monumental and urban investment associated with this foundation would provide a perfect historical context for dating the start of gold mining in the region. Furthermore, Martial's reference (Ep. 6.86) [6] to *Libicas Messis*, understood as the gold-producing areas of Iulia Libica, would fit perfectly within this historical and social framework, offering an important resource for the city's economic boom.

Both the reduced size and morphology of the mining structures at "Les Guilleteres," compared to the larger mines from the northwestern Iberian Peninsula, suggest that gold mining had an intense but not excessively long lifespan. In this regard, it should be noted that the city of Iulia Libica itself did not last long; from the late 2nd c. AD to early 3rd c. AD, the forum and excavated domestic sectors were abandoned [23]. This abandonment, which is also widely documented in other Roman cities in Hispania, aligns perfectly with the chronological age range obtained via OSL for the abandonment of the dated hydraulic structure. In other words, the period during which the OSL ages completely overlap corresponds with both the peak and decline of the city. By the early 4th c. AD, Llívia was no longer a Roman city.

Thus, we believe it is possible that the crisis and abandonment of the city of Iulia Libica coincided with the abandonment of the mines at Les Guilleteres—likely exploited as part of the territory and resources of this urban centre and ceased to be worked when the city fell into clear decline. While we cannot infer a direct cause and effect, it is possible that the complex hydraulic mining system developed by Roman technology in alluvial gold areas was no longer feasible in a context where the urban centre responsible for managing this resource also experienced significant decline.

From our perspective, our study suggests that the abandonment of the "Les Guilleteres d'All" mines likely dates to the late 2nd or early 3rd c. AD, a timeframe that also agrees with the abandonment of other gold mines in Hispania [24]. For example, by the second half of the 2nd c. AD, the great gold-mining region of the northwestern Iberian Peninsula already showed abandoned work zones and hydraulic networks, which clearly indicate reduced production. Therefore, although the OSL dating range for Les Guilleteres extends into the early 4th and even the 5th c. AD, we believe that, based on the specific chronology of Roman settlement in the area—especially the decline of Iulia Libica from the mid-2nd c. AD onward—and the general context of gold mining in Hispania, the decommissioning of the hydraulic structures in Les Guilleteres, and consequently the end of gold mining there, should be dated no later than the late 2nd or early 3rd c. AD.

7. Conclusions

For the first time, sediment layers associated with mining activities in Les Guilleteres d'All (Cerdanya, Girona) were dated using OSL, confirming that Cerdanya was a gold-mining area during Roman times. The archaeological excavation of an old water reservoir used for mining activities provided the opportunity for OSL dating, yielding an age for the end of gold mining there in the 3rd c. AD. This age is consistent with the literary and archaeological evidence collected from previous studies and coincides with the abandonment of the nearby Roman city of Iulia Libica, raising the question of whether the two events are linked.

Author Contributions: Conceptualisation, J.M.C. and O.O.V.; methodology, O.O.V. and J.S.-S.; validation, J.S.-S., J.M.C. and O.O.V.; formal analysis, J.S.-S.; investigation, J.M.C. and O.O.V.; writing—original draft preparation, J.S.-S. and O.O.V.; writing—review and editing, J.M.C. and O.O.V. All authors have read and agreed to the published version of the manuscript.

Funding: This research was developed in the frame of the research projects "Control, gestión y explotación del territorio en la Hispania romana: del modelo agrimensor al Paisaje Histórico", MINECO PID2021-122879OB-I00, funded by the Ministry of Science of Spain and "Paisatge i Territori a la Cerdanya Antiga-3" and the Generalitat of Catalonia, ARQ001SOL-109-2022. Jorge Sanjurjo-Sánchez also received funding from Xunta de Galicia through the Grupo Interdisciplinar de Patrimonio Cultural e Xeolóxico (CULXEO) (programme ED431B 2021/17).

Data Availability Statement: The original contributions presented in this study are included in the article. Further inquiries can be directed to the corresponding author.

Conflicts of Interest: The authors declare no conflicts of interest.

References

1. Hirt, A.M. *Imperial Mines and Quarries in the Roman World: Organizational Aspects, 27 BC–AD 235*; Oxford University Press: Oxford, UK, 2010.
2. Domergue, C. *Les Mines de la Péninsule Ibérique dans l'Antiquité Romaine*; Collection de l'École française de Rome 127; Ecole française de Rome: Rome, Italy, 1990.
3. Morera, J.; Olesti, O.; Oller, J.; Viladevall, M. El oro de los Ceretanos: Datos para una primera evaluación. In *Mines et Métallurgies Anciennes—Mélanges en L'honneur de Béatrice Cauuet*; Meunier, E., Hiriart, E., Fabre, J.M., Mauné, S., Tâmas, C., Eds.; Ausonius Éditions: Bordeaux, France, 2023; pp. 195–202.
4. Olesti, O.; Cauuet, B.; Oller, J.; Morera, J.; Viladevall, M. Les Guilleteres d'All (Cerdanya). *ERA Rev. Cerdana De Recer.* **2015**, *1*, 83–96.
5. Olesti, O.; García-Vuelta, O.; Montero, I. El taller metalúrgico del Castellot de Bolvir (II-I a.c.) y la presencia romana en el Pirineo. In *Presente y Futuro de los Paisajes Mineros del Pasado: Estudios Sobre Minería, Metalurgia y Poblamiento*; Pulido, L.G., Arboledas, L.A., Alarcón, E., Contreras, F., Eds.; University of Granada: Granada, Spain, 2018; pp. 243–249.
6. Olesti, O.; Andreu, R. Libicas messis?: Marcial i les mines d'or del pirineu oriental (Mart. Epigr. 6, 86). *Anu. Filologia. Antiqva Mediaev.* **2018**, *8*, 671–680.

7. Soto, A. A Roman Mining Landscape in the Pyrenees: How Does a High-Altitude Mining Landscape Compare with the Better-Known Mining Landscapes of Northwest Spain? Master's Thesis, Oxford University, Oxford, UK, 2025.
8. Viladevall, M.; Camacho, G.; Marturia, J.; Ponce, J.M. Los placeres auríferos de la llanura aluvial del río Segre y delta del río Ebro (NE de la Península Ibérica). In Proceedings of the Symopsium International sur les Gisements Alluviaux d'Or, La Paz, Bolivia, 1–5 June 1991; pp. 187–215.
9. Carreras, C.; Guitart, J.; Guàrdia, J. Iulia Libica (Llívia): Un municipium fronterizo en el corazón de los Pirineos. In Proceedings of the Small Towns, una Realidad Urbana en la Hispania Romana, Alicante, Spain, 26–28 October 2022; Volume 2, pp. 649–658.
10. Padró, J.; Montero, T.; Pons, E. Excavacions al jaciment romà del Pla de Prats (Prats de Cerdanya). In *Excavacions Arqueològiques d'Urgència a les Comarques de Lleida*; Generalitat de Catalunya: Barcelona, Span, 1989; pp. 133–161.
11. Feathers, J.K. Use of luminescence dating in archaeology. *Meas. Sci. Technol.* **2003**, *14*, 1493–1509. [CrossRef]
12. Wintle, A.G. Fifty years of luminescence dating. *Archaeometry* **2008**, *50*, 276–312. [CrossRef]
13. Sanjurjo-Sánchez, J. Dating Historical Buildings: An Update on the Possibilities of Absolute Dating Methods. *Int. J. Archit. Herit.* **2016**, *10*, 620–635. [CrossRef]
14. Fuchs, M.; Owen, L.A. Luminescence dating of glacial and associated sediments: Review, recommendations and future directions. *Boreas* **2008**, *37*, 636–659. [CrossRef]
15. Cong, L.; Wang, Y.; Zhang, X.; Chen, T.; Gao, D.; An, F. Radiocarbon and Luminescence Dating of Lacustrine Sediments in Zhari Namco, Southern Tibetan Plateau. *Front. Earth Sci.* **2021**, *9*, 640172. [CrossRef]
16. Brennan, B.J. Beta doses to spherical grains. *Radiat. Meas.* **2003**, *37*, 299–303. [CrossRef]
17. Murray, A.S.; Wintle, A.G. Luminescence dating of quartz using an improved single-aliquot regenerative-dose protocol. *Radiat. Meas.* **2000**, *32*, 57–73. [CrossRef]
18. Guerin, G.; Mercier, N.; Adamiec, G. Dose-rate conversión factors: Update. *Anc. TL* **2011**, *29*, 5–8. [CrossRef]
19. Prescott, R.R.; Hutton, J.T. Cosmic ray contributions to dose rates for luminescence and ESR dating: Large depths and long-term time variations. *Radiat. Meas.* **1994**, *23*, 497–500. [CrossRef]
20. Boyle, R.W. *Geochemical Prospecting for Thorium and Uranium Deposits*; Elsevier: Amsterdam, The Netherlands, 1982; 498p.
21. Galbraith, R.F.; Roberts, R.G.; Laslett, G.M.; Yoshida, H.; Olley, J.M. Optical dating of single and multiple grains of quartz from Jinmium rock shelter, northern Australia: Part I. Experimental design and statistical models. *Archaeometry* **1999**, *41*, 339–364. [CrossRef]
22. Ferrer, J.; Velaza, J.; Olesti, O. Nuevas inscripciones rupestres latinas de Oceja y los IIIIviri ibéricos de Iulia Lybica. *Dialogues D'histoire Ancienne* **2018**, *44*, 169–195.
23. Olesti, O.; Guárdia, J.; Maragall, M.; Nadal, J.; Mercadal, O.; Galbany, J. Controlling the Pyrenees: A macaque's burial from Late Antique Iulia Libica (Llívia). In *War and Warfare in Late Antiquity*; Sarantis, A., Christie, N., Eds.; BRILL: Leiden, The Netherlands, 2013; pp. 703–731.
24. Orejas, A. Metalla y minería en Hispania. In *Economía de la Hispania Romana: Paisajes de Producción y Dinámicas Comerciales*; Carreras, C., Molina, J., Olesti, O., Revilla, V., Eds.; Universitat de Barcelona: Barcelona, Spain, 2024; pp. 369–434.